Journal of the Meteorological Society of Japan, Vol. 93, No. 1, pp. 81−97, 2015
DOI:10.2151/jmsj.2015-006

Modulation of Northwest Pacific Tropical Cyclone Genesis by the Intraseasonal Variability

Haikun ZHAO

Pacific Typhoon Research Center, Key Laboratory of Meteorological Disaster of Ministry of Education, Nanjing University of Information Science and Technology, Nanjing, China

Xianan JIANG

Joint Institute for Region Earth System Science & Engineering, University of California, Los Angeles, U.S.A.

and

Liguang WU

Pacific Typhoon Research Center, Key Laboratory of Meteorological Disaster of Ministry of Education, Nanjing University of Information Science and Technology, Nanjing, China

(Manuscript received 8 May 2014, in final form 18 October 2014)

Abstract

The modulation of tropical cyclone (TC) genesis over the western North Pacific (WNP) by the intraseasonal variability (ISV) is investigated in this study. The two leading ISV modes, i.e., the 40-day Madden–Julian oscillation (MJO) and the 16-day quasi-biweekly oscillation, are found to exert significant impacts on TC genesis over the WNP. A majority of TC geneses over the WNP is found to occur during the period when both the modes are active, suggesting a joint influence of the two modes on TC genesis over the WNP.

The modulation of TC genesis over the WNP by the two leading ISV modes can be well depicted by the genesis potential index (GPI). Contributions of the four terms to the total GPI anomalies are further analyzed to determine the key factors involved in modulations of TC genesis by both of the ISV modes. Results indicate that while, in general, the low-level absolute vorticity and the mid-level relative humidity are the two most important factors affecting WNP TC genesis, relative roles of the four GPI factors also tend to be dependent on the ISV phases. This study provides further understanding of the ISV modulation of WNP TC genesis, which could benefit the intraseasonal prediction of the TC activity.

Keywords intraseasonal variability; Madden–Julian oscillation; quasi-biweekly oscillation; tropical cyclone genesis; western North Pacific

Corresponding author: Haikun Zhao, Pacific Typhoon Research Center, Key Laboratory of Meteorological Disaster of Ministry of Education, Nanjing University of Information Science and Technology, Nanjing 210044, China
E-mail: zhk2004y@nuist.edu.cn.

1. Introduction

Previous studies suggested that the tropical cyclone (TC) activity in the western North Pacific (WNP) is under the strong influence of various modes of natural climate variability, including interannual (Chan 2000; Chia and Ropelewski 2002; Wang and Chan 2002;

Zhao et al. 2010, 2011; Zhao et al. 2011; Li et al. 2012; Li and Zhou 2012; Wang et al. 2013a; Wang and Wang 2013) and decadal variations (Matsuura et al. 2003; Chan 2008; Liu and Chan 2008; Kim et al. 2010; Wang et al. 2012; Zhao et al. 2014; Zhao and Wu 2014), as well as the intraseasonal variability (ISV) (Nakazawa 1988; Liebmann et al. 1994; Wang and Zhou 2008; Kim et al. 2008; Chen et al. 2009; Liu et al. 2009; Sun et al. 2009; Pan et al. 2010; Tian et al. 2010; Mao and Wu 2010; He et al. 2011;Huang et al. 2011; Zhu et al. 2013; Li et al. 2013a, b).

The Madden–Julian Oscillation (MJO; Madden and Julian 1971) with a prevailing period of about 30–60 days is considered to be a dominant ISV mode influencing the TC activity on the intraseasonal time scale and has been widely documented in various studies (e.g., Gary 1979; Nakazawa 1988; Liebmann et al. 1994; Huang et al. 2011; Li et al. 2013a, b). During boreal summer, a prominent north-northeastward movement of the MJO mode over the Indian Ocean/western Pacific region has been widely documented (Yasunari 1979; Wang and Rui 1990; Hsu et al. 2004; Jiang et al. 2004). Meanwhile, a second dominant ISV mode with a prevailing period of about 10–30 days has also been identified over the Asian summer monsoon region and is often referred to as the quasi-biweekly oscillation (QBWO) (Krishnamurti and Bhalme 1976; Chen and Chen 1993; Kikuchi and Wang 2009; Chen and Sui 2010). Previous studies indicated that the kinetic energy of the QBWO is much stronger than that of the MJO over the WNP basin (Li and Zhou 1995), and thus, the QBWO can strongly affect the local TC activity (Wang et al. 2009; Li et al. 2013a, b).

Gray (1979) first found that global TC genesis occurs in clusters with 1–2 weeks of active TC genesis followed by 2–3 weeks of quiescence and further proposed a possible connection between the ISV and global TC activity. Over the WNP basin, an increase of TC genesis in the convective ISV phase and a decrease of TC genesis in the non-convective ISV phase can be clearly observed (Liebmann et al. 1994; Kim et al. 2008; Wang and Zhou 2008; Gao and Li 2011, 2012), which may be attributed either to modifications of the background mean flow by the ISV or to wave accumulation in terms of barotropic energy conversions (Maloney and Dickinson 2003; Mao and Wu 2010). Previous studies also reported that the ISV could exhibit significant impacts on TC genesis and movement over other oceans (e.g., Indian Ocean: Bessafi and Wheeler 2006; Ho et al. 2006; Kikuchi and Wang 2010; Eastern Pacific: Molinari et al. 1997; Maloney and Hartmann 2000a; Aiyyer and Molianri 2008; Jiang et al. 2012; Gulf and Mexico: Maloney and Hartmann 2000b; Mo et al. 2000; Higgins and Shi 2001; Atlantic Ocean: Maloney and Shaman 2008; Klotzbach 2010; Camargo et al. 2007; Australian Region: Ho et al. 2006), with a general consensus that the frequency of TC genesis is enhanced during the ISV convective period, while it is greatly damped when the ISV convection is suppressed.

While it has been well recognized that the ISV, especially the MJO mode, exerts pronounced modulations on the TC activity, the underlying physical mechanism on the intraseasonal variability of the WNP TC activity modulated by the MJO and QBWO modes remains poorly understood. Previous studies have shown some consistency between the ISV's modulation of large-scale environmental fields associated with TC genesis and its modulation of TC activities (Maloney and Hartmann 2000a, b; Hall et al. 2001; Bessafi and Wheeler 2006). Based on the analysis of cyclogenesis over the eastern North Pacific (ENP), Maloney and Hartmann (2000b) showed that TC genesis tends to be enhanced during the convectively active ISV phase. They further attributed the impact of the ISV on TCs to variations in the low-level relative vorticity and vertical wind shear (VWS) associated with the ISV. Anomalous low-level vorticity associated with the ISV is also found to be a key factor in modulating TC genesis over the ocean to the northwest of the Australian region (Hall et al. 2001). Meanwhile, impacts of the low-level vorticity and VWS associated with the ISV were found to be important for the intraseasonal modulation of cyclogenesis over the South Indian Ocean (Bessafi and Wheeler 2006). Over the WNP basin, a similar ISV modulation of TC activities was also investigated (Nakazawa 1988; Liebmann et al. 1994; Wang and Zhou 2008).

Recently, the TC genesis potential index (GPI), first proposed by Emanuel and Nolan (2004), was widely employed to quantitatively assess relative roles of several environmental factors affecting TC genesis. As will be discussed later, the GPI index involves four large-scale factors that play critical roles for TC genesis, i.e., the lower-tropospheric absolute vorticity, the mid-level moisture, VWS, and the potential intensity (PI). Camargo et al. (2009) illustrated that the GPI has considerable skills in representing global TC genesis on the intraseasonal time scale. They further suggested that the mid-level relative humidity (RH) is the most important factor that modulates the

TC genesis frequency, while the low-level absolute vorticity plays a secondary role. VWS and PI only have a very weak influence on TC genesis. These results are different from those in several other studies, in which dynamical factors—including the low-level vorticity and VWS—were found to play leading roles in modulating TC genesis (Maloney and Hartmann 2000a, b, Hall et al. 2001; Bessafi and Wheeler 2006; Wang and Zhou 2008). In addition, note that the first-position TC density field with nine grid-point smoothing (2.5° × 2.5° lat/lon grid from NCEP/NCAR; 1.125° × 1.125° lat/lon grid from ERA-40) was used by Camargo et al. (2009) to represent the TC genesis frequency over the global oceans. This method makes it difficult to describe the detailed features of TC genesis over a small ocean basin. In a recent study, Jiang et al. (2012) discussed the actual TC genesis during different ISV (10–90-day) phases over the ENP basin and re-examined roles of the four GPI variables associated with the ISV in modulating TC genesis. It was found that 600 hPa RH and 850 hPa vorticity are the two most important factors affecting TC genesis over the ENP basin, and VWS may also play an important role over a certain area of the ENP and during several specific MJO phases.

Most existing studies on the ISV–TC relationship focus on the impacts of the MJO mode, while studies on the influences of the QBWO on TC genesis remain limited. A recent analysis by Li et al. (2013a) examined impacts of both the QBWO and MJO on TC genesis over the WNP basin. Results suggested that the two ISV modes can distinctly modulate the TC activity over the WNP basin by changing the monsoon circulation and the associated environmental parameters. However, impacts of the large-scale environmental fields associated with the MJO or QBWO mode on TC genesis have not been quantitatively assessed in their study. As an extension to Li et al. (2013a), one major objective of the present study is to examine the key factors associated with the MJO and QBWO that affect WNP TC genesis based on the contributions of the four terms to the total GPI anomalies by following a similar approach as in Camargo et al. (2009) and Jiang et al. (2012). Results from this study will not only improve our understanding of ISV–TC relationships by considering both of the leading ISV modes but also provide useful information for the intraseasonal TC prediction over the WNP basin (Leory and Wheeler 2008).

This paper is organized as follows. Section 2 describes the datasets used in this study and the approach to identify the MJO and QBWO modes, including their phases and amplitudes. The dominant patterns and propagation characteristics of the MJO and the QBWO modes, as well as their impacts on TC genesis, over the WNP are investigated in Section 3. The key factors associated with the MJO and the QBWO in modulating WNP TC genesis are further explored in Section 4. Section 5 presents the summary.

2. Data and methodology

a. Data

In this study, rainfall observations during 1998–2012 derived from the Tropical Rainfall Measuring Mission (TRMM) version 3B42 (Huffman et al. 2007) are used to define the ISV phases over the WNP basin. TRMM 3B42 rainfall is a precipitation product based on multi-satellite and rain gauge analyses. It provides gridded precipitation estimates on a 3-h temporal resolution and a 0.25° spatial resolution in a zonal belt from 50°S to 50°N. The raw 3-hourly TRMM rainfall with a 0.25° spatial resolution is re-gridded into 1° × 1° daily data in this study.

The TC data used in this study is the best-track dataset from the Joint Warning Typhoon Center (JTWC), including the location and intensity of tropical storms and typhoons at a 6-h interval. Only those TCs that reach minimum tropical storm intensity (1-minute-averaged maximum sustained winds greater than 17.2 m s^{-1}) are considered in this study. Although TCs can occur all year round in the WNP basin, the analysis of this study is focused on the TC season from May to October, during which about 88 % of the annual total TC occurs. Although there are several organizations that maintain their own historical TC records for the WNP basin (e.g., JTWC, JMA-the Regional Specialized Meteorological Center of Japan Meteorological Agency, and CMA_STI-the Shanghai Typhoon Institute of China Meteorological Administration), previous studies suggested that the intensity records derived from these datasets were quite different (Wu et al. 2006; Emanuel et al. 2008; Ren et al. 2011; Wu and Zhao 2012). Chan (2008) suggested that the intensity records from JTWC are relatively reliable. In a recent study, Wu and Zhao (2012) further compared the intensity records that were derived dynamically with those from the three best-track datasets, including JTWC, CMA_STI, and JMA, and found that the TC intensity data from JTWC is relatively more reliable than the data from the other two best-track datasets. To explore the possible physical mechanisms responsible for the intraseasonal variability in the TC activity, daily

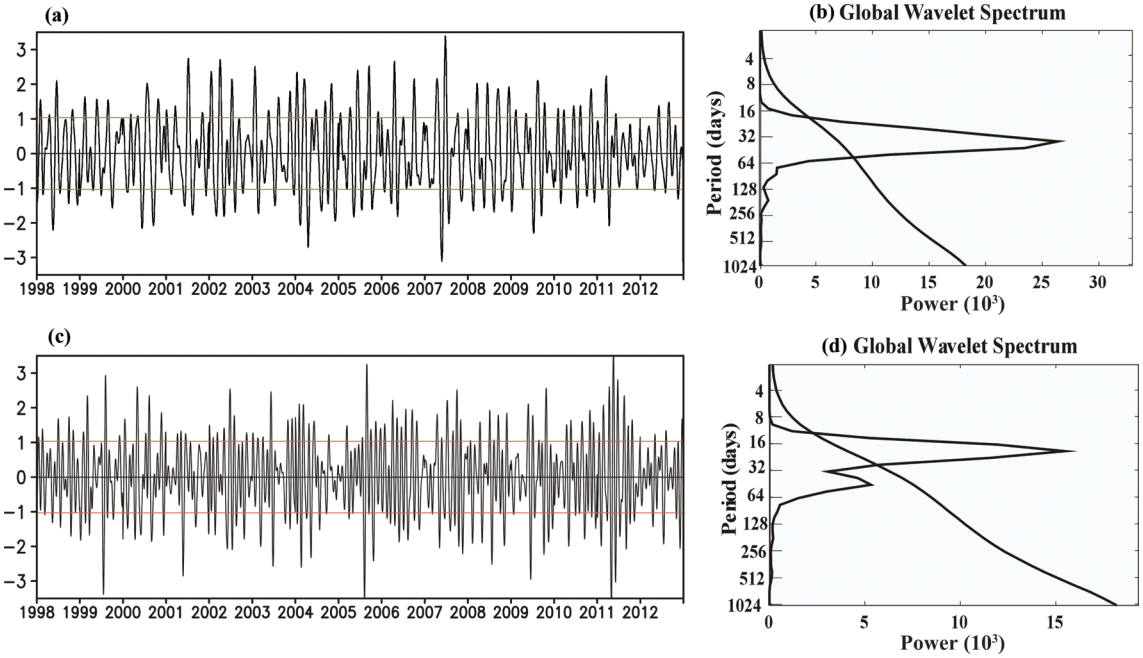

Fig. 1. Time series of principal components of the EEOF1 (a) and EEOF3 (c) modes of 10–90-day bandpass-filtered TRMM rainfall anomalies during boreal summer (May–October) for the period of 1998–2012, with corresponding global wavelet spectra shown in (b) and (d), respectively.

atmospheric variables, including winds, RH, temperature, and sea surface temperature (SST), during 1998–2012 are analyzed. These variables are extracted from the recent ECMWF (European Centre for Medium-Range Weather Forecasts) ERA-Interim reanalysis (Dee et al. 2011), which has a horizontal resolution of 1.5° × 1.5°.

b. Methodology

The extended empirical orthogonal function (EEOF) (Weare and Nasstrom 1982) is used in this study. The EEOF analysis has a unique feature that it focuses on a sequential spatiotemporal evolution by the extension of the EOF analysis to a segment of consecutive times, and thus, it is more appropriate to document a propagating phenomenon. With the appropriate series of successive time points included, a pair of the first two EEOFs can represent a half cycle of the ISV (Lau and Chan 1985, 1986), whereas with longer series of time points included, the first EEOF alone can represent a whole cycle (Kayano and Kousky 1999) or more cycles (Waliser et al. 2003, 2004) of the ISV.

Following Jiang et al. (2012), an EEOF analysis of daily 10–90-day bandpass-filtered TRMM rainfall anomalies during the period of 1998–2012 are conducted to extract the leading ISV modes over the WNP. Temporal lags of 31 days are adopted, and the domain [20°S–30°N, 60°E–180°E] is selected for EEOF analyses. Similar to the results of Jiang et al. (2012), in this study, two leading ISV modes over the WNP are identified by the two leading pairs of the EEOF modes. These two leading pairs, i.e., EEOF1 and EEOF2, and EEOF3 and EEOF4, represent the propagating features of the two leading ISV modes. According to the variance explained by each EEOF mode based on the formula by North et al. (1982), it is found that the first two leading pairs of the EEOF stand out from the remaining EEOF modes and are also well separated from each other. The two leading EEOFs contribute about 5.8 % of the total anomalous variances of the bandpass-filtered daily data with lags of 31 days. The second pair of EEOFs explains about 3.3 % of the total variances (Figure not shown). Time series of the principal components (PCs) of EEOF1 and EEOF3 are illustrated in Fig.1. Further spectral analysis of corresponding PCs suggests a prevailing period of about 40 days and 20 days for the first and second leading modes, respectively. Overall, the first two leading EEOF modes of the observed daily rainfall anomalies capture the dominant MJO mode

(40-day ISV mode) and QBWO mode (16-day ISV mode). Based on lagged regression patterns of the bandpass-filtered TRMM rainfall for the EEOF-1 and EEOF-3 modes, pronounced eastward and northward propagation for the MJO mode and northwestward propagation for the QBWO were observed during the boreal summer over the WNP basin (figures not shown). The time evolution patterns associated with the two leading modes derived by the regressed patterns of PCs of the two leading EEOF modes are in great agreement with those obtained in many previous studies and particularly those based on a generally similar approach but using a combination of the EOF of OLR and 850hPa u wind by Lee et al. (2013). All these results further lend confidence to the EEOF method used in this study to isolate the two leading ISV modes over the WNP basin.

Following a similar method adopted in Wheeler and Hendon (2004), the first and second leading PCs are used to determine the daily MJO and QBWO amplitudes and phases (ranging from 1 to 8), respectively. Then, the eight phases are obtained, and each available day is assigned into one of these eight phases. In this study, an additional phase, Phase 9, is used to denote a weak phase for the MJO or QBWO mode. Phase 9 includes days when the amplitude is less than 1 (MJO: Sqrt ($PC1^2 + PC2^2$) < 1.0; QBWO: Sqrt ($PC3^2 + PC4^2$) < 1.0). Composite analyses for the observed rainfall are conducted by averaging the 10–90-day bandpass-filtered rainfall anomalies over each MJO (QBWO) phase based on the selected strong MJO (QBWO) events (MJO strong events: Sqrt ($PC1^2 + PC2^2$) ≥ 1.0; QBWO strong events: Sqrt ($PC3^2 + PC4^2$) ≥ 1.0) during the period of 1998–2012. The TC data are then binned into one of these eight phases, in addition to a weak phase, e.g., each TC is assigned to a specific phase for both the MJO and QBWO modes.

3. Dominant patterns of the two ISV modes and their modulations of TC genesis

Figure 2a shows the standard deviation of 10–90-day filtered rainfall (shaded) anomalies and WNP TC genesis positions during the active TC season from 1998 to 2012. Pronounced ISV activity over the WNP basin is clearly shown in Fig. 2a. The region with maximum intraseasonal variances of rainfall extends from 110°E to 150°E and from 10°N to 25°N, which coincides with the main development region (MDR) of WNP TC genesis. Further analysis indicates that variances for the MJO and QBWO modes show a similar spatial pattern with the maxima over the

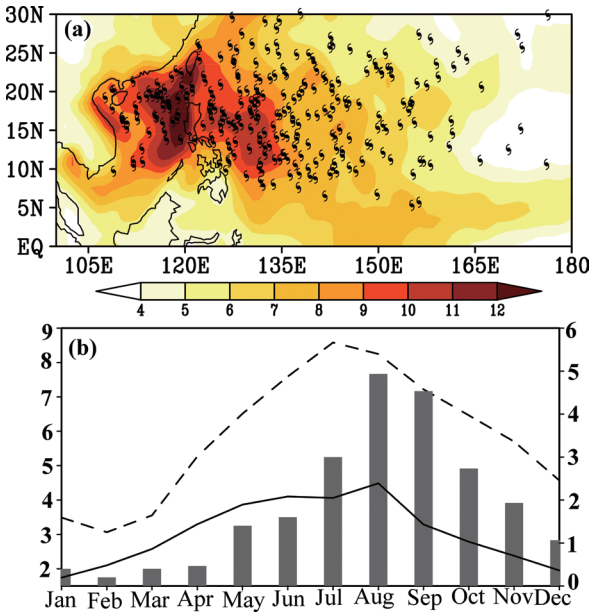

Fig. 2. (a) Standard deviation of 10–90-day filtered TRMM rainfall anomalies (shaded) and TC genesis locations (black dots) during boreal summer (May–October) for the period of 1998–2012 and (b) seasonal evolution of TC genesis counts (bar) and domain averaged STD of 10–30-day (dashed line) and 30–90-day (solid line) filtered rainfall over the region [10°N–25°N]*[110°E–150°E].

MDR (figures not shown). Moreover, in agreement with the results of Li and Zhou (1995), the QBWO exhibits larger amplitude in variance than the MJO mode (Fig. 2b). Figure 2b also illustrates the seasonal evolution of the standard deviations (STD) of TRMM rainfall on both 10–30-day and 30–90-day bands averaged over 10°N–25°N and 110°E–150°E. It is clearly shown that the active TC occurrence over the WNP during boreal summer is closely associated with the vigorous activity of both the MJO and QBWO, suggesting a possible role of the ISV in affecting WNP TC genesis.

Figure 3 illustrates the observed composite rainfall anomalies and TC genesis locations during a life cycle of the MJO. In agreement with previous studies (Kim et al. 2008; Huang et al. 2011; Li et al. 2013a), the MJO mode, which propagates both eastward and northward during the boreal summer, exerts strong modulations on TC genesis over the WNP basin. Generally, TC genesis is more frequent during the period of enhanced convection compared to that

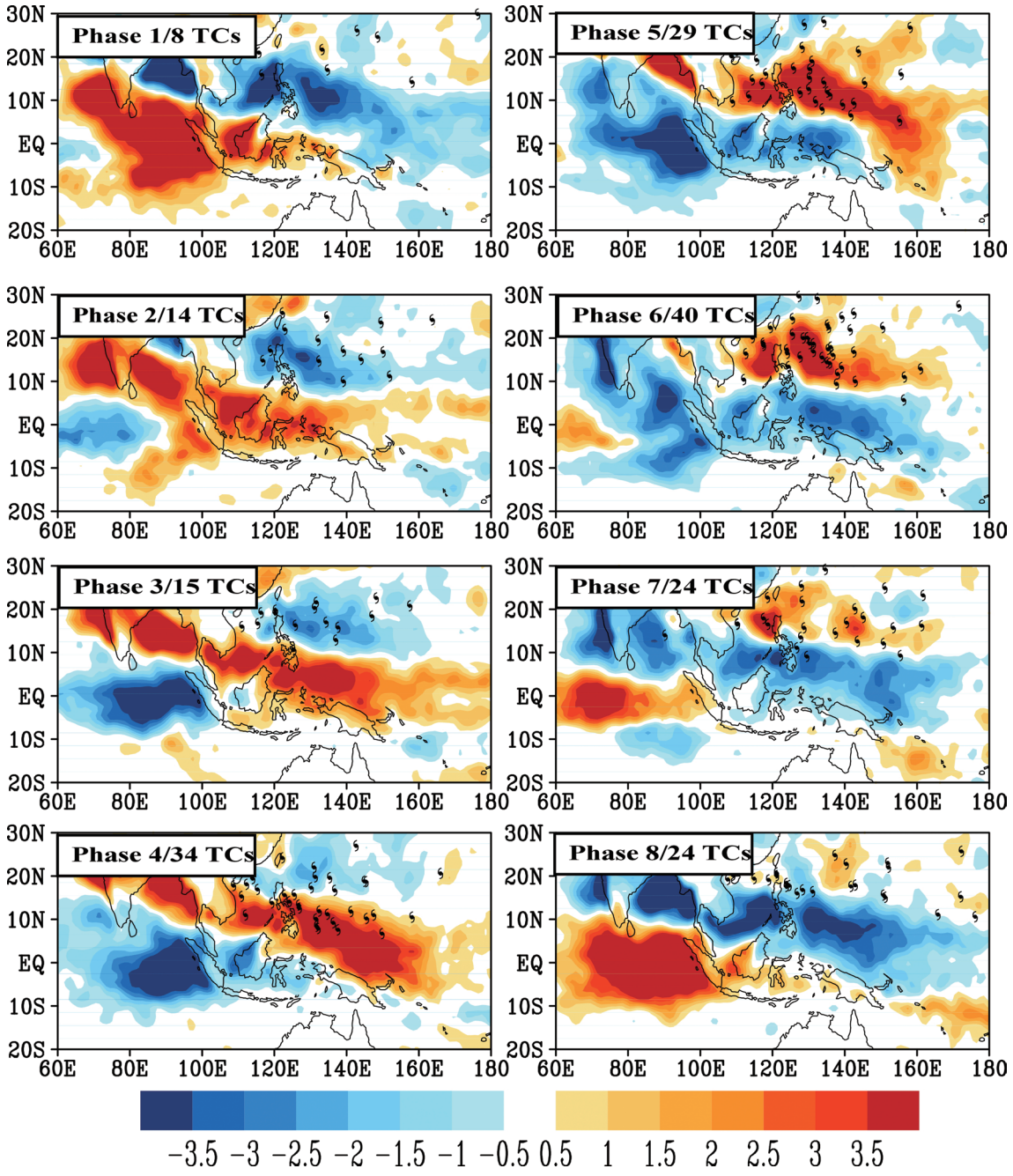

Fig. 3. Observed composite anomalous rainfall pattern (shaded with the color bar on the bottom) associated with TC genesis over the WNP basin from 1998 to 2012 during different MJO phases.

during the suppressed ISV convection period. From Phases 4 to 8, the TC genesis zone exhibits a clear migration coupled with the northward movement of the enhanced MJO convection. Compared with the active convection period during Phases 4–6, the inactive MJO convection period over the WNP basin during Phases 1–3 is generally consistent with the significantly decreased TC genesis during the same period. A similar composite analysis for anomalous rainfall and TC genesis during the life cycle of the

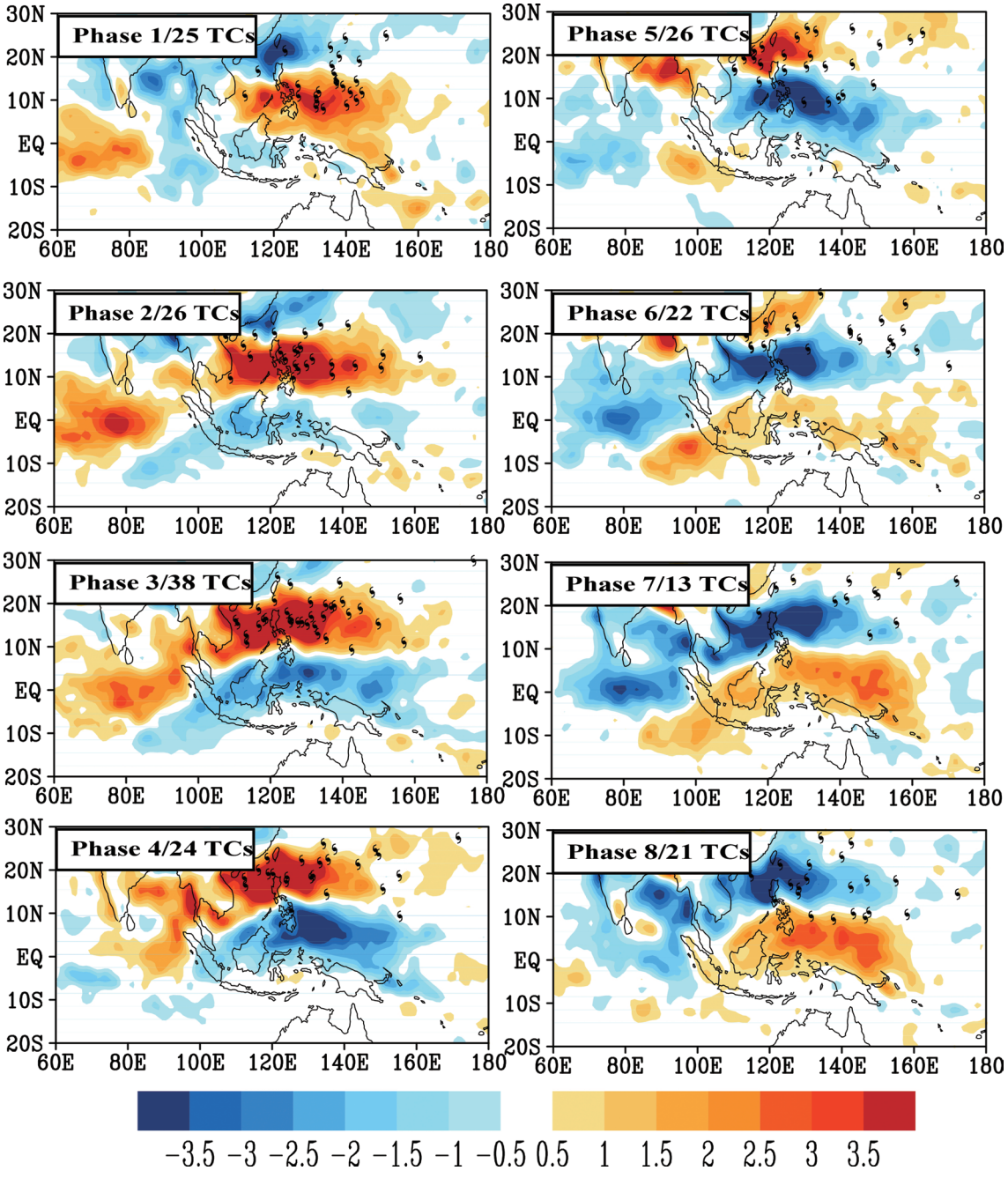

Fig. 4. Same as in Fig. 3, but for composite patterns during different QBWO phases.

QBWO is also performed, and the results are shown in Fig. 4. In contrast to the northeastward migration of the MJO, the QBWO is characterized by the northwestward movement of convection, which is also in accord with an obvious northwestward shift of the TC genesis location.

Figure 5 further illustrates strong impacts of the MJO and QBWO on WNP TC genesis by displaying the TC genesis rate (i.e., the ratio of the TC genesis counts to the number of total days) as a function of the phase corresponding to each ISV mode. As shown in Fig. 5a, considerably more TCs form during the

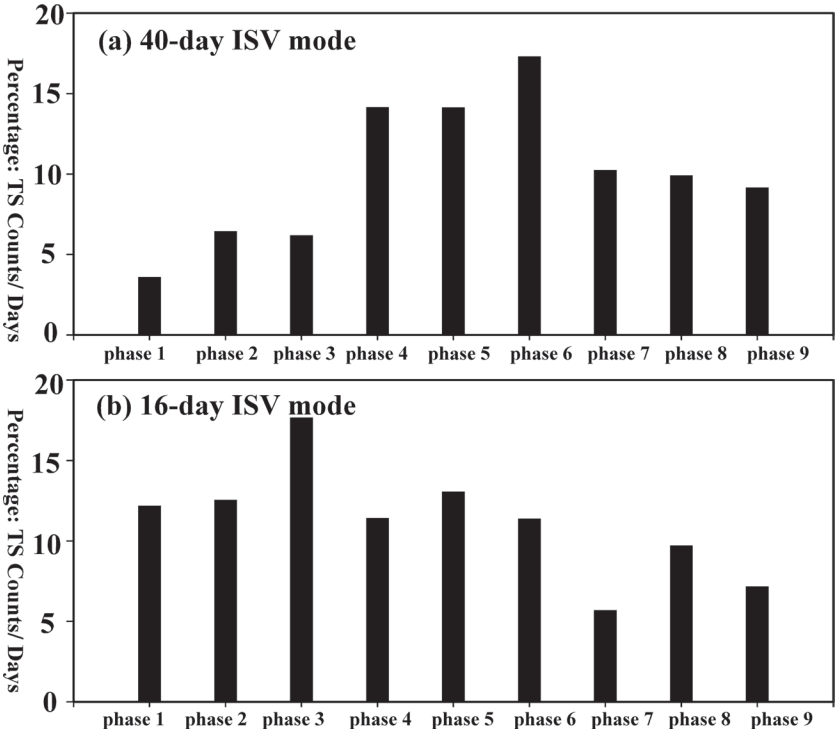

Fig. 5. TC genesis rate (TC counts/ ISO days) during the different MJO (a) and QBWO (b) phases over the WNP basin. Phases 1 to 8 for the strong MJO and QBWO phases, while phase "9" represents weak MJO or QBWO phase. The strong MJO and QBWO phases are identified by the amplitudes of sqrt(PC1*PC1 + PC2*PC2) ≥ 1.0 and sqrt(PC3*PC3 + PC4*PC4) ≥ 1.0, respectively.

MJO convectively active Phases 4, 5, and 6, whereas much less genesis rate is observed during the MJO Phases 1, 2, and 3 when suppressed convection prevails over the WNP MDR. A relatively small TC genesis rate is also found during the weak MJO period (phase 9). Similar results are found for the QBWO that higher TC genesis rates are found during phases 1–5 with a peak value occurring at QBWO Phase 3; these results are illustrated in Fig. 5b. A much smaller TC genesis rate is found during Phase 7, which is comparable to the TC genesis rate during the weak Phase 9.

Further analyses suggest that a majority of TCs generated over the WNP can be modulated by both the MJO and QBWO modes. As shown in Fig. 6, about 47 % of the total TCs (127 out of 273) over the WNP basin occur when both of the ISV modes are active. In contrast, only 6 % (17 out of 273) of the total TCs form when both of the ISV modes are inactive. When considering the contribution from each individual ISV mode, 22 % (61 out of 273) of the total TCs occur during the period when only the MJO model is active and 25 % (68 out of 273) when only the QBWO is active. These results clearly suggest that the QBWO, in addition to the MJO mode, also plays an important role in WNP TC genesis. This is in agreement with the results shown in Fig. 4 that the QBWO can significantly modulate the TC genesis location. It is also found that the impact of the QBWO on TC genesis is more localized than that of the MJO on TC genesis because of the QBWO's relatively small spatial scale and alternating positive and negative convection anomalies. This also explains why the modulation of the QBWO on TC genesis over the entire WNP is not as strong as that of the MJO mode (Figs. 5a, b).

Further evidence of modulations of TC genesis by both the MJO and QBWO modes is presented in Fig. 7. For each summer day during the period of 1998–2012, the ISV phases for both the MJO and QBWO modes are determined as previously described in the manuscript based on the leading PCs corresponding to the two ISV modes. When the 40-day ISV (QBWO) mode is strong, namely, Sqrt ($PC1^2$ + $PC2^2$) ≥ 1.0

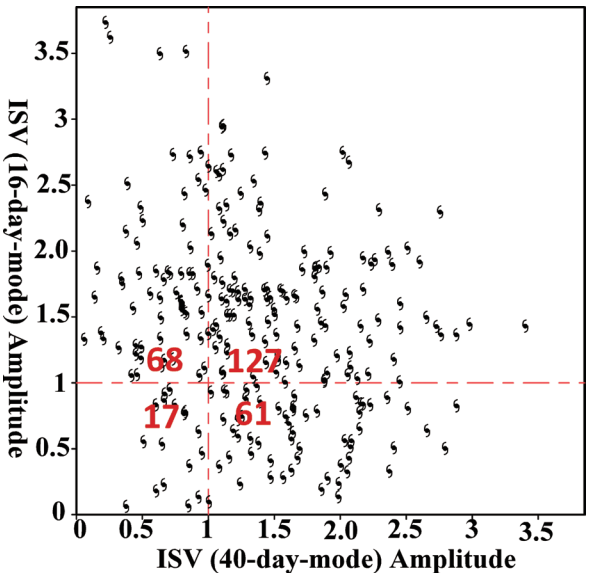

Fig. 6. Scatter plot of the amplitude of the MJO (abscissa) and QBWO (ordinate) associated with each of a total of 273 TCs over the WNP during the TC season from 1998 to 2012.

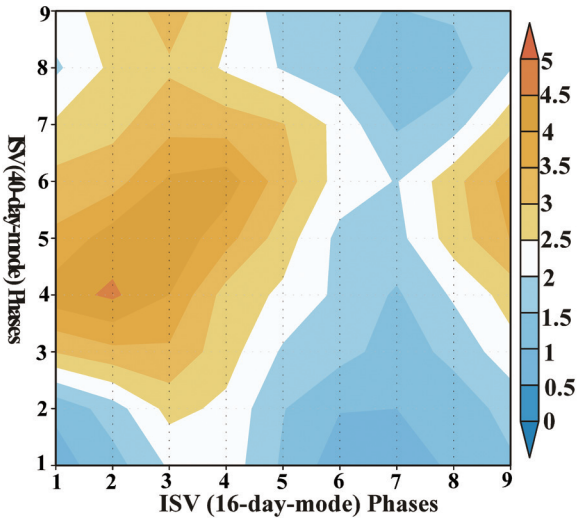

Fig. 7. TC genesis counts as a function of the MJO (abscissa) and QBWO (ordinate) phases during the TC season from 1998 to 2012.

(Sqrt ($PC3^2 + PC4^2$) ≥ 1.0), a specific phase ranging from 1 to 8 is defined based on the pair of PC1 and PC2 (PC3 and PC4). Otherwise, if the ISV mode is weak on that day, a phase number of 9 is then specified for this ISV mode. Then, the total TC genesis counts over the WNP during these 13 summers are binned into the combinations of eight phases (1–8), in addition to a weak phase (9), for the ISV modes. Figure 7 shows the TC genesis counts as a function of both the MJO and QBWO phases. For example, the value when $x = 1$ and $y = 2$ in Fig. 7 represents the total TC genesis counts that occurred when the MJO mode was in Phase 1 and the QBWO mode was in Phase 2, respectively, during the 13 summers from 1998 to 2010. It clearly indicates that there is more TC formation during the active phases of both of the leading ISV modes, i.e., Phases 3–7 of the MJO and 1–4 of the QBWO. More interestingly, a tilted zone with maximum TC genesis counts is evident in Fig.7, corresponding to the MJO Phases 3–6 and QBWO Phases 1–4, suggesting the joint influence on the TC genesis of the two ISV modes. Abovementioned results are in general agreement with previous studies (Kim et al. 2008; Wang et al. 2009; Huang et al. 2011; Li et al. 2013a), which have found a basin-wide increase (decrease) in the WNP TC genesis frequency during the strong (weak) MJO phase, as well as a localized impact of the QBWO.

As illustrated in Hsu et al. (2008), the rainfall associated with TCs may contribute to the ISV variance. Additional EOF analyses of the 10–90-day bandpass-filtered rainfall anomalies during these non-TC days (1468 days) from 1998 to 2012 are also performed. It is found that the two dominant ISV modes identified by the leading EOFs are basically similar to those based on EEOF during the full period of 15 summers (figure not shown). Apparently, the MJO and QBWO modes over the WNP basin revealed by the EEOF analyses represent two intrinsic low-frequency convective variability modes that are independent of TC activities. Therefore, the results discussed above about the relationship between the two dominant ISV modes and WNP TC geneses are robust.

4. Factors controlling the intraseasonal TC genesis

In this section, the key factors associated with the two dominant ISV modes in modulating TC genesis over the WNP basin are further explored by utilizing a GPI analysis (Emanuel and Nolan 2004), following a similar approach as in Jiang et al. (2012). The GPI is defined as follows:

$$GPI = \frac{\left|10^5 \xi\right|^{3/2}}{\eta} \frac{\left(\frac{H}{50}\right)^3}{\gamma} \frac{\left(\frac{V_{pot}}{70}\right)^3}{\varphi} \frac{(1+0.1\cdot V_{shear})^{-2}}{s}, \quad (1)$$

where ζ is the 850 hPa absolute vorticity (s^{-1}), H is the 600 hPa RH (%), V_{pot} is PI (m s^{-1}), and V_{shear} is computed as the wind difference between 850 hPa and 200 hPa (m s^{-1}). The terms η, γ, φ, and S represent the GPI components and are associated with 850 hPa absolute vorticity, 600 hPa RH, PI, and VWS. PI can be computed according to the algorithm of Bister and Emanuel (2002), who consider SST and vertical profiles of temperature and specific humidity in the troposphere, which are defined by the expression as follows:

$$V_{pot}{}^2 = \frac{T_s}{T_o}\frac{C_k}{C_D}(CAPE^* - CAPE^b)\,, \tag{2}$$

where T_s is SST, T_o is the mean outflow temperature at the level of neutral buoyancy, C_k is the exchange coefficient for enthalpy, C_D is the drag coefficient, $CAPE^*$ is the convective available potential energy (CAPE) for an air parcel at the radius of maximum winds, and $CAPE^b$is the CAPE of boundary layer air (Bister and Emanuel 2002; Camargo et al. 2007).

Figure 8 shows the evolution of anomalous GPI along with TC genesis during the MJO life cycle. Corresponding to the observed rainfall anomalies displayed in Fig. 3, the positive (negative) GPI anomalies are generally in association with the active (inactive) phase of convection. The majority of TCs occur over regions where the positive GPI anomalies are present. Note that a small number of TCs can also be found over regions with the negative GPI anomalies (e.g., Phases 2), which can be attributed to other factors that are not included in Eq. (1) or not associated with the MJO. Similarly, Fig. 9 illustrates the evolution of the GPI anomalies and TC genesis associated with the QBWO. It is found that TC genesis during the QBWO phases can also be generally depicted by the GPI anomalies. Again, a small number of TCs occur over the regions with the negative GPI anomalies, e.g., Phase 8 (Fig. 9).

Since the evolution of anomalous GPI patterns can reasonably well represent TC genesis associated with both the MJO and QBWO (Figs. 8, 9), relative importance of the four terms involved in the GPI calculation are further examined. For clarifying purposes, each term contributing to the GPI anomalies, η, γ, φ, ,and S in Eq. (1), can be decomposed into two components: a climatological annual cycle component and a departure from the climate. The latter contains variability on various time scales. Thus, the GPI anomalies associated with the MJO or QBWO can be decomposed into four linear terms, the relative role of which can be further explored by keeping one item realistic while the other three terms specified with their summer mean climatological values. Moreover, the contributions of nonlinear terms can also be examined by high-order variances of two or more terms.

Figure 10a displays contributions of the four terms to the GPI anomalies during different MJO phases. The positive GPI anomalies are found over the period from the MJO Phases 3 to 6, while the negative GPI anomalies are evident during Phases 7 and 8 and also during Phases 1 and 2. Further analysis shows that PI has a weak influence on the GPI anomalies, while both 600 hPa RH and 850 hPa absolute vorticity make significant contributions to the MJO composite GPI anomalies. However, contributions of these terms to the total GPI anomalies are different and depend on different phases of the MJO.

During the MJO Phases 4 and 5, the 600 hPa RH and 850 hPa vorticity are the two most important terms that contribute to the maximum positive GPI anomalies, while VWS makes a major negative contribution to the GPI anomalies. The 850 hPa absolute vorticity and 600 hPa RH remain to be the most important factors contributing to the maximum positive GPI anomalies during Phase 6, whereas PI and VWS contribute to the negative GPI anomalies with comparable amplitudes. Note that during the MJO Phase 3, the total positive GPI anomalies are mainly caused by the ISV of PI, while other three factors have little impact. Moreover, it is found that contributions of these four factors to the negative GPI anomalies during Phases 7 and 8 and also 1 and 2 largely mirror those to the positive GPI anomalies from sPhases 3 to 6. During Phases 1–8, the nonlinear term makes only minor contributions to the GPI anomalies.

Similar analyses are conducted for the total GPI anomalies over the QBWO life cycle (Fig. 10b). Note that the amplitudes of contributions of these factors during the QBWO are generally smaller than those during the MJO. Similar to the results for the MJO Phases 4 and 5, from the QBWO Phases 3 to 6, the mid-level RH makes the largest contribution to the QBWO composite GPI anomalies. The low-level absolute vorticity and VWS tend to be the second important factors with positive and negative contributions, respectively; a relatively small contribution is made by PI. During Phase 7 of the QBWO, the negative GPI anomalies are mainly caused by the 850 hPa absolute vorticity and PI, while VWS shows a positive effect on the total GPI anomalies. During Phase 8, the low-level absolute vorticity and 600 hPa RH make the largest contribution to the total negative GPI anomalies, while the contribution of the total nega-

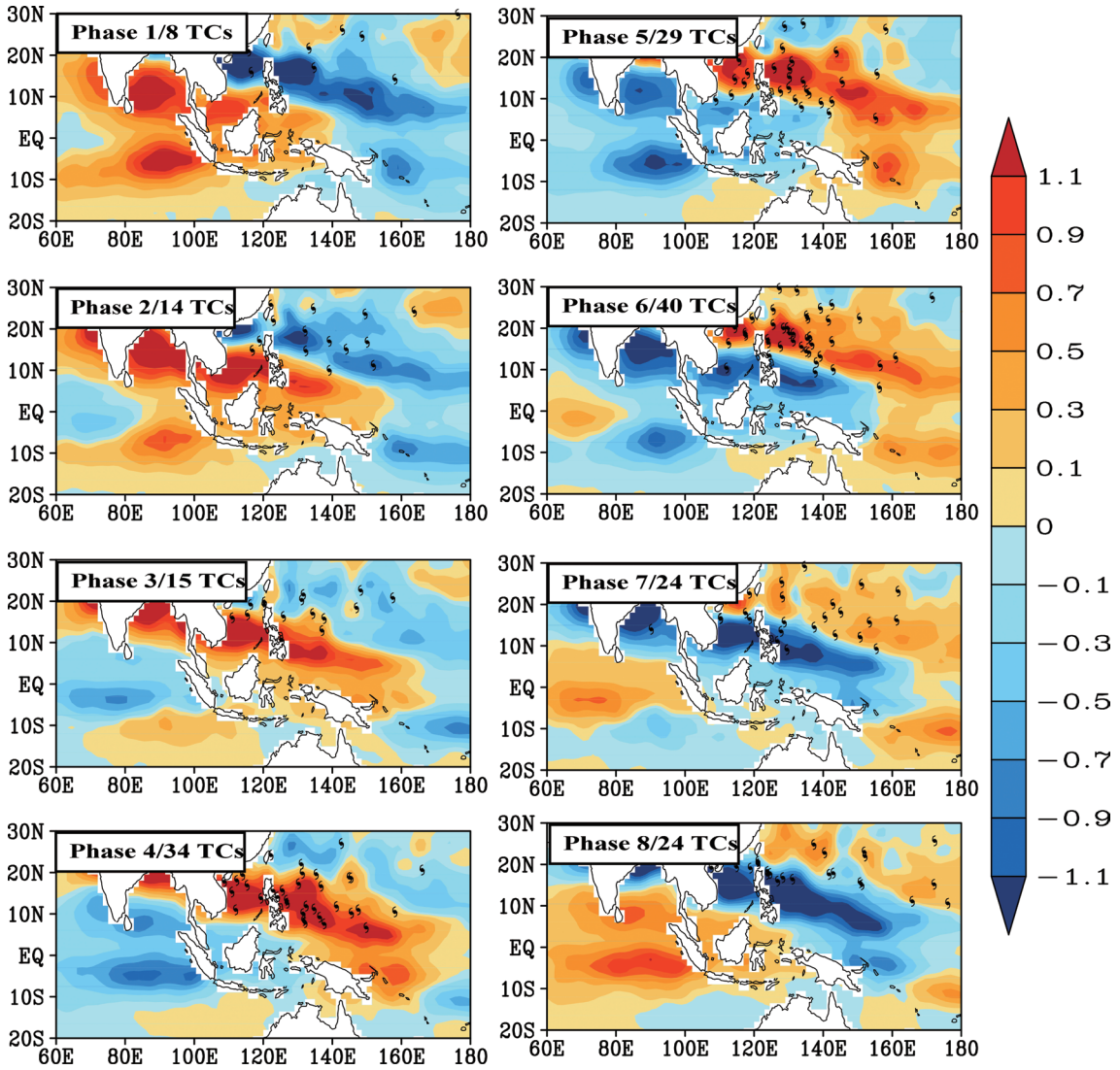

Fig. 8. Composite GPI anomalies (shaded, see color scale on the right) at different MJO phases along with the TC genesis events based on observation during the period of 1998–2012.

tive GPI anomalies are significantly reduced by the impact of VWS. During Phases 1 and 2, the influence of the four factors to the negative GPI anomalies is not negligible, where the 850 hPa absolute vorticity and 600 hPa RH contribute to the total negative GPI anomalies, while contributions of PI and VWS reduce the GPI anomalies. Note that the nonlinear contribution to the observed GPI anomalies associated with the QBWO is more important than that with the MJO, especially during the QBWO Phases 2–5.

3. The above results further suggested that the impacts of the ISV on TC genesis over the WNP basin are largely due to the changes in large-scale factors. Further examinations found that during the active phase of the MJO mode over the western Pacific (e.g., Phases 4–6), cyclonic low-level circulation as a result of Rossby wave responses and enhanced mid-level RH is evidently associated with enhanced ISV convection. These two factors contribute to the positive GPI anomalies and play positive roles for TC genesis. On the other hand, the enhanced anomalous southwesterly winds in the lower troposphere corresponding to the enhanced ISV convection tend to increase the total wind speed considering the

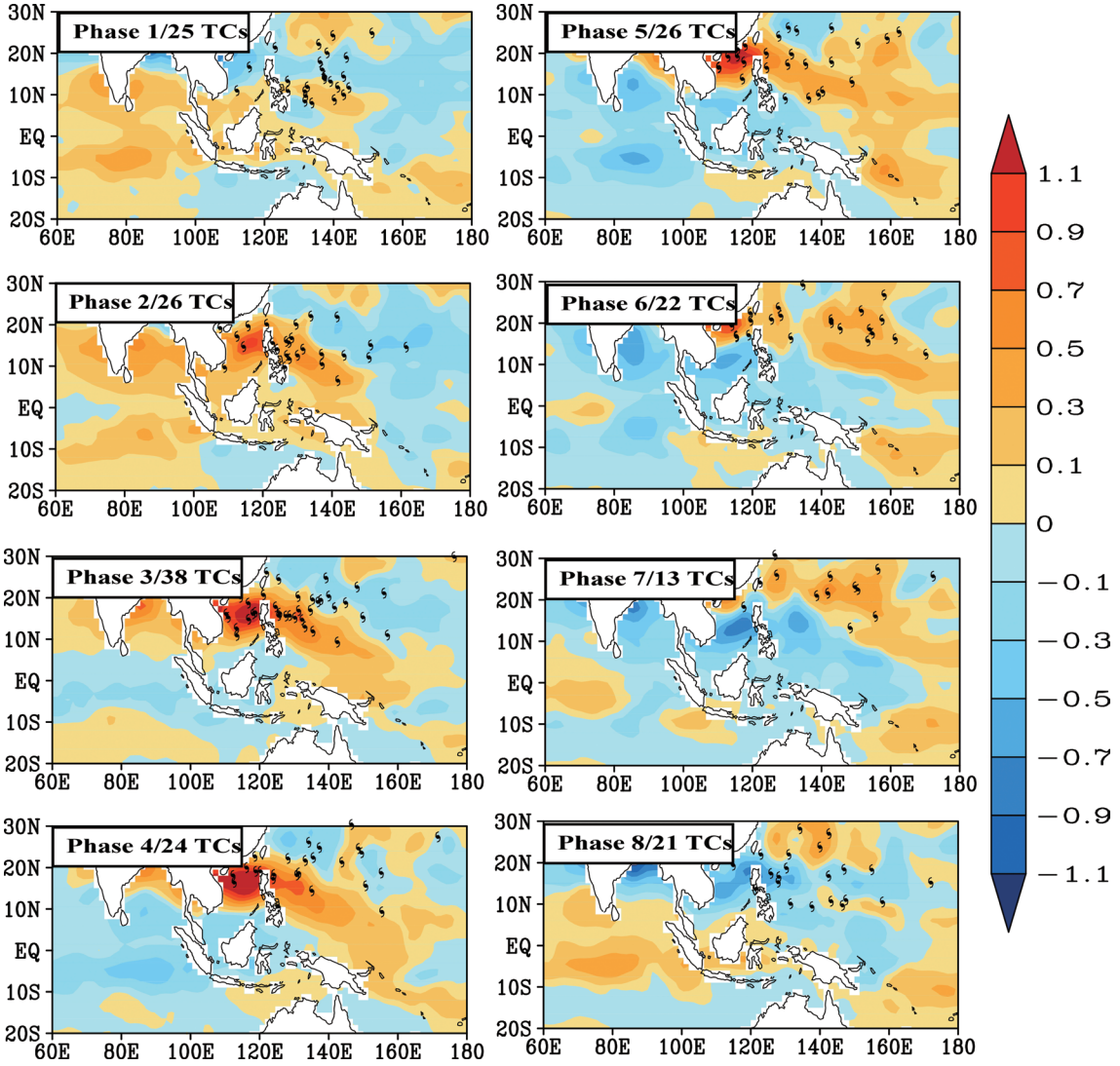

Fig. 9. Same as Fig. 8, but for the QBWO.

low-level southwesterly mean monsoonal circulation. Therefore, it increases VWS during the active ISV phase, i.e., positive anomalies, and disfavors TC genesis. As for PI, which is mainly linked to SST, becomes largely negative during the enhanced phase of the MJO mode as results of increased surface evaporation and the reduction of solar radiation because of cloudiness; thus, it also plays a negative role for TC genesis during the active ISV phases. Similar results are also found for the QBWO mode.

5. Summary

In this study, the impacts of the two leading intra-seasonal variability modes, i.e., the MJO and QBWO, on TC genesis over the WNP during the active TC season from 1998 to 2012 are re-examined with a particular emphasis on the joint impact of these two ISV modes. In agreement with previous studies (Liebmann et al. 1994; Wang and Zhou 2008; Camargo et al. 2009; Wang et al. 2009; Huang et al. 2011; Li et al. 2013a), it is illustrated that while both the MJO and QBWO can modulate TC genesis over the WNP, a majority of the TC genesis events occur when both of the ISV modes are active.

Following Jiang et al. (2012), the key environmental factors associated with the two dominant

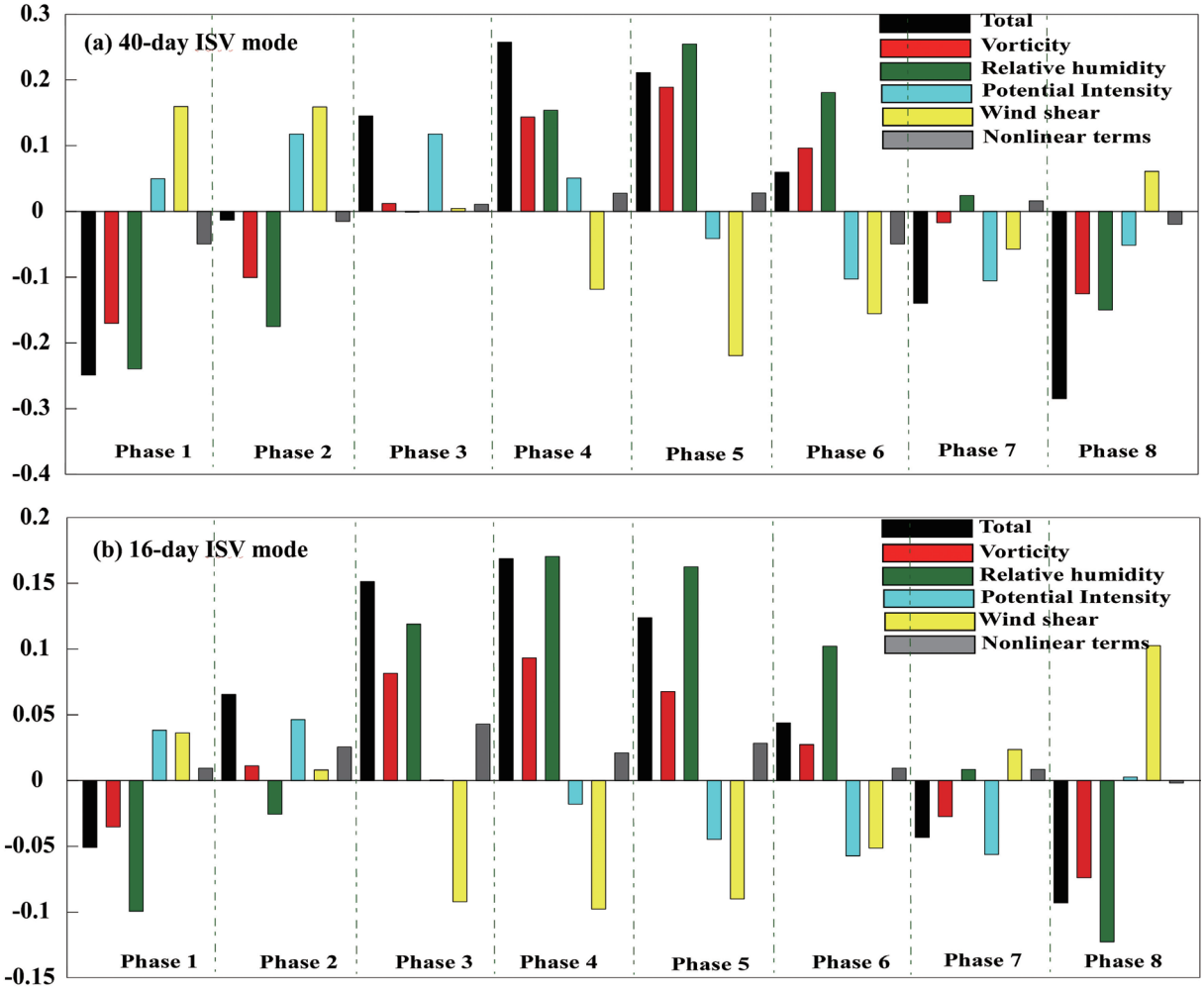

Fig. 10. Contributions of the four terms to the total observed GPI anomalies over the WNP basin as a function of the MJO (a) or QBWO (b) phase.

ISV modes in modulating TC genesis over the WNP basin are further explored by the GPI analysis, which is proposed by Emanuel and Nolan (2004). Consistent with a previous study by Camargo et al. (2009), it is found that anomalous GPI patterns associated with the WNP MJO and QBWO can well depict the modulations of TC genesis by these two ISV modes. We further examine the relative roles of four GPI environmental variables associated with the MJO and QBWO. Their contributions to the total GPI anomalies during the MJO and QBWO life cycles are analyzed.

Camargo et al. (2009) suggested that mid-level humidity and low-level vorticity tend to be the two most important contributors to the MJO composite GPI anomalies based on similar analyses for the global oceans. With a focus on the WNP basin, the present study reveals that the impacts of these factors are different and depend on the MJO and QBWO phases, which are similar to those over the ENP basin (Jiang et al. 2012). Both the 850 hPa absolute vorticity and 600 hPa RH make major contributions to the observed active WNP TC genesis during all MJO and QBWO phases. Meanwhile, VWS and the 850-hPa absolute vorticity also contribute to the total GPI anomalies during the specific QBWO and MJO phases. Nonlinear terms for the total GPI anomalies associated with the QBWO tend to be more important than those with the MJO. While details on these nonlinear processes warrant further investi-

gation, this result is largely consistent with previous studies that synoptic-scale activity also feedbacks to the ISV (Zhou and Li 2010; Hsu and Li 2011a, b; Rong et al. 2011). In particular, the ISV–TC relationship as suggested by the composite results for the entire TC season as shown in this study can be generally observed in composites for the early (May–June) and later (July–August) summer season. However, it is worth mentioning that the ISV modulation of TC in early summer is stronger than that in late summer. About 69 % of total TCs are formed during the active ISV phases (e.g., Phases 4–7) in early summer, while about 45 % of total TCs are generated when the ISV is active during late summer.

Although the impacts of environmental factors modulated by ISV on WNP TC genesis is similar to that over the ENP basin in Jiang et al. (2012). The observed modulations of TC genesis over the ENP basin by the large-scale ISV are represented better than those over the WNP basin. For example, some WNP TCs occur over regions with negative rainfall anomalies during phase 2 of the MJO (Fig. 3). This suggests that the physical mechanism controlling TC genesis over the WNP basin could be more complex than that over the ENP basin. In addition to the impact of the MJO and QBWO modes, previous studies suggested that the monsoon trough and subtropical high also play significant roles in affecting WNP TC genesis (Wu et al. 2012; Molinari and Vollaro 2013; Wang et al. 2013a; Wang et al. 2013b); these need further investigations.

Acknowledgments

This research was jointly sponsored by the National Natural Science Foundation of China (41305050), the National Natural Science of Foundation of China (41275093), the National Natural Science Foundation of China (41375098), the National Natural Science Foundation of China (41475091), the National Basic Research Program of China (2013CB430103, 2015CB452803), the project of the specially appointed professorship of Jiangsu Province, the foundation of the Jiangsu Government Scholarship for overseas studies, and the Priority Academic Program Development of Jiangsu Higher Education Institutions (PAPD).This study is the Earth System Modeling Center Contribution Number 018.

References

Aiyyer, A., and J. Molinari, 2008: MJO and tropical cyclogenesis in the Gulf of Mexico and eastern Pacific: Case study and idealized numerical modeling. *J. Atmos. Sci.*, **65**, 2691–2704.

Barrett, B. S., and L. M. Leslie, 2009: Links between tropical cyclone activity and Madden–Julian oscillation phase in the North Atlantic and northeast Pacific basins. *Mon. Wea. Rev.*, **137**, 727–744.

Bessafi, M., and M. C. Wheeler, 2006: Modulation of South Indian Ocean tropical cyclones by the Madden–Julian oscillation and convectively coupled equatorial waves. *Mon. Wea. Rev.*, **134**, 638–656.

Camargo, S. J., K. A. Emanuel, and A. H. Sobel, 2007: Use of a genesis potential index to diagnose ENSO effects on tropical cyclone genesis. *J. Climate*, **20**, 4819–4834.

Camargo, S. J., M. C. Wheeler, and A. H. Sobel, 2009: Diagnosis of the MJO modulation of tropical cyclogenesis using an empirical index. *J. Atmos. Sci.*, **66**, 3061–3074.

Chan, J. C. L., 2000: Tropical cyclones activity over the western North Pacific associated with El Niño and La Niña events. *J. Climate*, **13**, 2960–2972.

Chan, J. C. L., 2008: Decadal variations of intense typhoon occurrence in the western North Pacific. *Proc. R. Soc. A.,* **464**, 249–272.

Chand, S. S., and K. J. E. Walsh, 2010: The influence of the Madden-Julian oscillation on tropical cyclone activity in the Fiji region. . *J. Climate*, **23**, 868–886.

Chen, G., and R. Huang, 2009: Dynamical effects of low frequency oscillation on tropical cyclogenesis over the western North Pacific and the physical mechanisms. *Chinese J. Atmos. Sci.*, **33**, 205–214 (in Chinese).

Chen, G., and C. H. Sui, 2010: Characteristics and origin of quasi—biweekly oscillation over the western North Pacific during boreal summer. *J. Geophys. Res.*, **115**, D14113, doi:10.1029/2009JD013389.

Chen, T.-C., and J.-M. Chen, 1993: The 10–20-day mode of the 1979 Indian monsoon: Its relation with the time variation of monsoon rainfall. *Mon. Wea. Rev.*, **121**, 2465–2482.

Chia, H. H., and C. F. Ropelewski, 2002: The interannual variability in the genesis location of tropical cyclones in the northwest Pacific. *J. Climate*, **15**, 2934–2944.

Emanuel, K. A., and D. S. Nolan, 2004: Tropical cyclone activity and the global climate system. *Preprints, 26th Conf. on Hurricanes and Tropical Meteorology*, Miami, FL, Amer. Meteor. Soc., 10A.2.

Emanuel, K., R. Sundararajan, and J. Williams, 2008: Hurricanes and global warming: Results from downscaling IPCC AR4 simulations. *Bull. Amer. Meteor. Soc.*, **89**, 347–367.

Gao, J., and T. Li, 2011: Factors controlling multiple tropical cyclone events in the western North Pacific. *Mon. Wea. Rev.*, **139**, 885–894.

Gao, J., and T. Li., 2012: Interannual variation of multiple tropical cyclone events in the western North Pacific. *Adv. Atmos. Sci.*, **29**, 1279–1291.

Gray, W. M., 1979: Hurricanes: Their formation, structure and likely role in the tropical circulation. *Meteorology Over Tropical Oceans*. Shaw, D. B. (ed.), 155–218.

Hall, J. D., A. J. Matthews, and D. J. Karoly, 2001: The modulation of tropical cyclone activity in the Australian region by the Madden–Julian oscillation. *Mon. Wea. Rev.*, **129**, 2970–2982.

He J., Q. Wan, Z. Guan, A. Lin, and L. Wang, 2011: Comparative analysis on active and inactive years of tropical cyclone activities with relevance to intraseasonal oscillations in Asian to western Pacific region in boreal summer. *Chinese J. Atmos. Sci.*, **27**, 22–30 (in Chinese).

Held, I. M., and M. Zhao, 2011: The response of tropical cyclone statistics to an increase in CO_2 with fixed sea surface temperatures. *J. Climate*, **24**, 5353–5364.

Higgins, R. W., and W. Shi, 2001: Intercomparison of the principal modes of interannual and intraseasonal variability of the North American monsoon system. *J. Climate*, **14**, 403–417.

Ho, C. H., J. H. Kim, J. H. Jeong, H. S. Kim, and D. L. Chen, 2006: Variation of tropical cyclone activity in the South Indian Ocean: El Niño-Southern Oscillation and Madden-Julian Oscillation effects. *J. Geophys. Res.*, **111**, D22101, doi: 10.1029/2006JD007289.

Hsu, H.-H., C.-H. Weng, and C.-H. Wu, 2004: Contrasting characteristics between the northward and eastward propagation of the intraseasonal oscillation during the boreal summer. *J. Climate*, **17**, 727–743.

Hsu, H.-H., C.-H. Hung, A.-K. Lo, C.-C. Wu, and C.-W. Hung, 2008: Influence of tropical cyclones on the estimation of climate variability in the tropical western North Pacific. *J. Climate*, **21**, 2960–2975.

Hsu, P. C., T. Li, and C.-H. Tsou, 2011a: Interactions between boreal summer intraseasonal oscillations and synoptic-scale disturbances over the western North Pacific. Part I: Energetics diagnosis. *J. Climate*, **24**, 927–941.

Hsu, P. C., and T. Li, 2011b: Interactions between boreal summer intraseasonal oscillations and synoptic-scale disturbances over the western North Pacific. Part II: Apparent heat and moisture sources and eddy momentum transport. *J. Climate*, **24**, 942–961.

Huang, P., C. Chou, and R. H. Huang, 2011: Seasonal modulation of tropical intraseasonal oscillations on tropical cyclone geneses in the western North Pacific. *J. Climate*, **24**, 6339–6352.

Huffman, G. J., R. F. Adler, D. T. Bolvin, G. Gu, E. J. Nelkin, K. P. Bowman, E. F. Stocker, and D. B. Wolff, 2007: The TRMM multi-satellite precipitation analysis: Quasi-global, multi-year, combined-sensor precipitation estimates at fine scale. *J. Hydrometeor.*, **8**, 33–55.

Jiang, X., T. Li, and B. Wang, 2004: Structures and mechanisms of the northward propagating boreal summer intraseasonal oscillation. *J. Climate*, **17**, 1022–1039.

Jiang, X., M. Zhao, and D. E. Waliser, 2012: Modulation of tropical cyclones over the eastern Pacific by the intraseasonal variability simulated in an AGCM. *J. Climate*, **25**, 6524–6538.

Kayano, M. T., and V. E. Kousky, 1999: Intraseasonal (30–60 day) variability in the global tropics: Principal modes and their evolution. *Tellus*, **51**, 373–386.

Kikuchi, K., and B. Wang, 2010: Formation of tropical cyclones in the northern Indian Ocean associated with two types of tropical intraseasonal oscillation modes. *J. Meteor. Soc. Japan*, **88**, 475–496.

Kim, J. H, C.-H. Ho, H. S. Kim, C. H. Sui, and S. K. Park, 2008: Systematic variation of summertime tropical cyclone activity in the western North Pacific in relation to the Madden-Julian oscillation. *J.Climate,* **21**, 1171–1191.

Kim, J.-H., C.-H. Ho, and P.-S. Chu, 2010: Dipolar redistribution of summertime tropical cyclone genesis between the Philippine Sea and the northern South China Sea and its possible mechanisms. *J. Geophys. Res.*, **115**, D06104, doi:10.1029/2009JD012196.

Klotzbach, P. J., 2010: On the Madden–Julian oscillation–Atlantic hurricane relationship. *J. Climate*, **23**, 282–293.

Krishnamurti, T. N., and H. N. Bhalme, 1976: Oscillations of a monsoon system. Part I: Observational aspects. *J. Atmos. Sci.*, **33**, 1937–1954.

Lau, K. M, and P. H. Chan, 1985: Aspects of the 40–50 day oscillation during the northern winter as inferred from outgoing long wave radiation. *Mon. Wea. Rev.,* **113**, 1889–1909.

Lau, K. M, and P. H. Chan, 1986: Aspects of the 40–50 day oscillation during the northern summer as inferred from outgoing long wave radiation. *Mon. Wea. Rev.,* **114**, 1354–1367.

Lee, J.-Y., B. Wang, M. Wheeler, X. Fu, D. Waliser, and I.-S. Kang, 2013: Real-time multivariate indices for the boreal summer intraseasonal oscillation over the Asian summer monsoon region. *Climate Dyn.*, **40**, 493–509.

Leroy, A., and M. C. Wheeler, 2008: Statistical prediction of weekly tropical cyclone activity in the Southern Hemisphere. *Mon. Wea. Rev.*, **136**, 3637–3654.

Li, R. C. Y., and W. Zhou, 2013a: Modulation of western North Pacific tropical cyclone activity by the ISO. Part I: Genesis and intensity. *J.Climate*, **26,** 2904–2918.

Li, R. C. Y., and W. Zhou, 2013b: Modulation of western North Pacific tropical cyclone activity by the ISO. Part II: Tracks and landfalls. *J. Climate*, **26**, 2919–2930.

Liebmann, B., H. H. Hendon, and J. D. Glick, 1994: The relationship between tropical cyclones of the western Pacific and Indian Oceans and the Madden–Julian oscillation. *J. Meteor. Soc. Japan*, **72**, 401–412.

Li, C. Y., and Y. P. Zhou, 1995: On quasi-two-week (10-20-day) oscillation in the tropical atmosphere. *Chinese J.*

Atmos. Sci., **19**, 435–444 (in Chinese).

Li, C. Y., and W. Zhou, 2012: Changes in western Pacific tropical cyclones associated with the El Nino-Southern oscillation cycle. *J. Climate*. **25**, 5864–5878.

Li, C. Y., W. Zhou, J. C. L. Chan, and P. Huang, 2012: Asymmetric modulation of the western North Pacific cyclogenesis by the Madden-Julian oscillation under ENSO conditions. *J. Climate*, **25**, 5374–5385.

Liu, G., S. Sun, Q. Zhang, et al. 2009: Characteristics of the intraseasonal oscillation of intertropical convergence zone and its influence on the periodical tropical cyclogenesis. *Chinese J. Atmos. Sci.*, **33**, 879–889 (in Chinese).

Liu, K. S., and J. C. L. Chan, 2008: Interdecadal variability of western North Pacific tropical cyclone tracks. *J. Climate*, **21**, 4464–4476.

Madden, R. A., and P. R. Julian, 1971: Detection of a 40–50 day oscillation in the zonal wind in the tropical Pacific. *J. Atmos. Sci.*, **28**, 702–708.

Maloney, E. D., and D. L. Hartmann, 2000a: Modulation of hurricane activity in the Gulf of Mexico by the Madden–Julian oscillation. *Science*, **287**, 2002–2004.

Maloney, E. D., and D. L. Hartmann, 2000b: Modulation of eastern North Pacific hurricanes by the Madden–Julian oscillation. *J. Climate*, **13**, 1451–1460.

Maloney, E. D., and J. Shaman, 2008: Intraseasonal variability of the West African monsoon and Atlantic ITCZ. *J. Climate*, **21**, 2898–2918.

Mao, J., and G. Wu, 2010: Intraseasonal modulation of tropical cyclogenesis in the western North Pacific: A case study. *Theor. Appl. Climatol.*, **100**, 397–411.

Molinari, J., and D. Vollaro, 2013: What percentage of western North Pacific tropical cyclones form within the monsoon trough? *Mon. Wea. Rev.*, **141**, 499–505.

North, G. R., T. L. Bell, R. F. Cahalan, and F. J. Moeng, 1982: Sampling errors in the estimation of empirical orthogonal functions. *Mon. Wea. Rev.*, **110**, 699–706.

Matsuura, T., M. Yumoto, and S. Iizuka, 2003: A mechanism of interdecadal variability of tropical cyclone activity over the western North Pacific. *Climate. Dyn.*, **21**,105–117.

Mo, K. C., 2000: The association between intraseasonal oscillations and tropical storms in the Atlantic basin. *Mon. Wea. Rev.*, **128**, 4097–4107.

Molinari, J., D. Knight, M. Dickinson, D. Vollaro, and S. Skubis, 1997: Potential vorticity, easterly waves, and eastern Pacific tropical cyclogenesis. *Mon. Wea. Rev.*, **125**, 2699–2708.

Nakazawa, T., 1988: Tropical super clusters within intraseasonal variations over the western Pacific. *J. Meteor. Soc. Japan*, **66**, 823–839.

Pan, J., C. Y. Li, and J. Song, 2010: The modulation of Madden-Julian oscillation on typhoons in the northwestern Pacific Ocean. *Chinese J. Atmos. Sci.*, **34**, 1059–1070 (in Chinese).

Ren, F., J. Liang, G. Wu, W. Dong, and X. Yang, 2011: Reliability analysis of climate change of tropical cyclone activity over the western North Pacific. *J. Climate*, **24**, 5887–5898.

Rong, X., R. Zhang, T. Li, and J. Su, 2011: Upscale feedback of high-frequency winds to ENSO. *Quart. J. Roy. Meteor. Soc.*, **137**, 894–907.

Sun, Z., J. Mao, and G. Wu, 2009: Influences of intraseasonal oscillations on the clustering of tropical cyclone activities over the western North Pacific during boreal summer. *Chinese J. Atmos. Sci.*, **33**, 950–9581.

Tian, H., C. Y. Li, and H. Yang, 2010: Modulation of typhoon genesis over the western North Pacific by intraseasonal oscillation. *Chinese J. Trop. Meteor.*, **26**, 283–292 (in Chinese).

Waliser, D. E., R. Murtugudde, and L. E. Lucas, 2003: Indo-Pacific Ocean response to atmospheric intraseasonal variability: 1. austral summer and the Madden-Julian oscillation. *J. Geophys. Res.*, **108**, 3160, doi:10.1029/2002JC001620.

Waliser, D. E., R. Murtugudde, and L. E. Lucas, 2004: Indo-Pacific Ocean response to atmospheric intraseasonal variability: 2. Boreal summer and the intraseasonal oscillation. *J. Geophys. Res.*, **109**, C03030, doi: 10.1029/2003JC002002.

Wang, B., and H. Rui, 1990: Synoptic climatology of transient tropical intraseasonal convection anomalies—1975–1985. *Meteor. Atmos. Phys.,* **44**, 43–61.

Wang, B., and J. C. Chan, 2002: How strong ENSO events affect tropical storm activity over the western North Pacific. *J. Climate*, **13**, 1517–1536.

Wang, B., and X. Zhou, 2008: Climate variability and predictability of rapid intensification in tropical cyclones in the western North Pacific. *Meteor. Atmos. Phys.*, **99**, 1–16.

Wang, B., B. Xiang, and J.-Y. Lee, 2013a: Subtropical High predictability establishes a promising way for monsoon and tropical storm predictions. *PNAS*, **110**, 2718–2722.

Wang, C., and X. Wang, 2013: Classifying El Niño Modoki I and II by different impacts on rainfall in southern China and typhoon tracks. *J. Climate*, **26**, 1322–1338.

Wang, L., G. H. Chen, and R. H. Huang, 2009: The modulation of quasi-biweekly oscillat ion tropical cyclone activity over the western North Pacific. *Chinese J. Atmos. Sci.*, **33**, 416–424 (in Chinese).

Wang, X., W. Zhou, C. Li, and D. Wang, 2012: Effects of the East Asian summer monsoon on tropical cyclones genesis over the South China Sea on an interdecadal timescales. *Adv. Atmos. Sci*., **29**, 249–262.

Wang, X., W. Zhou, C. Li, and D. Wang, 2013b: Comparison of the impact of two types of El Niño on tropical cyclone genesis over the South China Sea. *Int. J. Climatol*., **34**, 2651–2660.

Wheeler, M. C., and H. H. Hendon, 2004: An all-season real-time multivariate MJO index: Development of an index for monitoring and prediction. *Mon. Wea. Rev.*,

132, 1917–1932.

Wu, L., Z. Wen, R. Huang, and R. Wu, 2012: Possible linkage between the monsoon trough variability and the tropical cyclone activity over the western North Pacific. *Mon. Wea. Rev.,* **140**, 140–150.

Wu, L., and H. Zhao, 2012: Dynamically derived tropical cyclone intensity changes over the western North Pacific. *J. Climate*, **25**, 89–98.

Wu, M.-C., K.-H. Yeung, and W.-L. Chang, 2006: Trends in western North Pacific tropical cyclone intensity. *Eos, Trans. Amer. Geophys. Union*, **87**, 537–538.

Yasunari, T., 1979: Cloudiness fluctuations associated with the northern hemisphere summer monsoon. *J. Meteor. Soc. Japan*, **57**, 227–242.

Zhao, H. K., L. G. Wu, and W. C. Zhou, 2010: Assessing the influence of the ENSO on tropical cyclone prevailing tracks in the western North Pacific. *Adv. Atmos. Sci.*, **27**, 1361–1371.

Zhao, H. K., L. G. Wu, and W. C. Zhou, 2011: Interannual Changes of tropical cyclone intensity in the Western North Pacific. *J. Meteor. Soc. Japan*, **125**, 89–101.

Zhao, H. K., and L. G. Wu, 2014: Inter-decadal shift of the prevailing tropical cyclone tracks over the western North Pacific and its mechanism study. *Meteor. Atmos. Phys.*, **125**, 89–101.

Zhao, H. K., L. G. Wu, and R. F. Wang, 2014: Decadal variations of intense tropical cyclones over the western North Pacific during 1948–2010. *Adv. Atmos. Sci.*, **31**, 57–65.

Zhou, C., and T. Li, 2010: Upscale feedback of tropical synoptic variability to intraseasonal oscillations through the nonlinear rectification of the surface latent heat flux. *J. Climate*, **23**, 5738–5754.

Zhu, L., Y. Wang, and Z. Yin, 2013: Relationship between tropical cyclone activity over the South China Sea and tropical ISO propagation. *Chinese J. Trop. Meteor.,* **29**, 727–738 (in Chinese).